Section A-Research paper

Synthesis, Spectroscopic Characterization, Biological activities, DFT Computation, and Molecular docking Studies of Azomethines.

Minakshee A. Todarwal[1], Rakesh S. Sancheti[1], Arvind M. Patil[1], Jaiprakash N Sangshetti[2], Manoj. G. Damale[3], Ratnamala S. Bendre[4*]

1. Department of Chemistry, KKHA Arts, SMGL Commerce, and SPHJ Science College,Chandwad, 423101(Maharashtra) India.
2. Department of pharmaceutical Chemistry Y.B Chavan College of Pharmacy, Aurangabad, 431001(Maharashtra) India.
3. Department of pharmaceutical Chemistry, Shrinath College of Pharmacy, Aurangabad, 431001(Maharashtra) India.
4. Department of Chemistry, KBC, North Maharashtra University, Jalgaon, 425002(Maharashtra) India

Corresponding Author
Email-bendrers@gmail.com.
Address- Department of Chemistry, KBC, North Maharashtra University, Jalgaon, 425002 (Maharashtra) India
Mobile No.:8788300846

Abstract-

Azomethine derivatives were synthesized and analyzed using mass spectrometry as well as 1H and 13C-NMR techniques. These derivatives were investigated for their potential antioxidant, antibacterial, antifungal, and antimalarial properties. Remarkably, azomethine P2 exhibited substantial antibacterial efficacy against S. aureus (25 µg/ml) and achieved an impressive maximum docking score of -5.188 kcal/mol. In the case of antifungal activity, both P1 and P6 (250 µg/ml) demonstrated remarkable potency against C. albicans. Meanwhile, compound P5 showcased noteworthy antimalarial activity with an IC50 value of 0.29 g/ml. On the other hand, azomethine P7 exhibited significant antioxidant activity with an IC50 value of 14.26 g/ml. Molecular docking analysis highlighted that compounds P1, P2, and P5 exhibited the highest level of activity among all the tested compounds. Through Density Functional Theory (DFT) studies, it was observed that the substantial dipole moment values of compounds P1 and P5 facilitated robust intramolecular interactions. This characteristic contributed to their effective binding to specific target proteins. Conversely, due to its lower dipole moment and higher energy gap, compound P3 emerged as the most stable derivative in the set. Combining biological and computational investigations, it was determined that P5 stood out as the most biologically active molecule among all the compounds studied. This comprehensive exploration sheds light on the

potential of these azomethine derivatives for various applications and underscores the importance of their distinct structural and energetic properties.

Keywords-

Schiff base, antibacterial, antioxidant, antimalarial, molecular docking.

Introduction-

Microbial infections and drug-resistant bacteria are the main causes of death worldwide. Resistance to antibiotics is a severe health issue that threatens humanity, as determined by the World Health Organization (WHO). Hence, the synthesis of novel compounds with the potential to serve as promising antimicrobial agents, aimed at addressing the challenge of microbial resistance, stands as a significant subject captivating the attention of bioorganic chemistry [1–3]. Staphylococcus aureus is a bacterial strain resistant to penicillin family medications. In the community, Staphylococcus *aureus* causes serious illnesses. These pathogenic bacteria cause pneumonia and diseases of the blood and skin [4]. Muthukumar et al. reported (E)-4-(4-bromobenzylidene)amino) synthesized from 4-bromobenzaldehyde and sulphanilamide has potent antibacterial activity [5]. Rajimon et al. synthesized azomethine from salicylaldehyde, and chloroanilines demonstrated greater efficacy against S.aureus bacteria and moderate activity against *C.albicans* fungus than commercial amoxicillin[6]. Bendre et al. reported (Z)−2-(4-(1,1,1,3,3,3-hexafluoro-2-hydroxypropyl-2-yl) phenyl)imino) methyl) - 6 isopropyl-3-methyl phenol) has potent antibacterial action against *Staphylococcus aureus* [7]. Azomethine (-C=N) is important in showing potency against microorganisms[8]. A category of reactive oxygen species (ROS) present in the biological system includes hydroxyl radicals, superoxide radicals, singlet oxygen, and hydrogen peroxide. These ROS have been shown to have a negative impact on nucleic acids, proteins, lipids, DNA, and carbohydrates, potentially leading to the start of a variety of disorders. Cancer, atherosclerosis, ageing, hair loss, inflammation, immunological suppression, diabetes, and neurodegenerative illnesses are examples of such conditions[9]. Within living organisms, antioxidant compounds play a crucial role in averting damage to macromolecules and cells by intervening with free radical molecules[10]. Therefore, the significance of searching for antioxidants has noticeably better in recent years [11]. Synthetic antioxidising agents were cheaper and more effective than natural ones, so they have been widely used in recent years [12]. The hydroxyl-substituted aromatic azomethine derivatives are more effective antioxidants and offer great promise as possible medicinal agents for treating disorders caused by free radical damage [13]. *Plasmodium falciparum, Plasmodium malariae, Plasmodium ovale,* and *Plasmodium vivax* parasites cause malaria in humans. The addition of azomethine (-C=N) functionality boosts the efficiency of antimalarial drugs. [14, 15 16]. Azomethines are an important class in the medicinal and

pharmaceutical fields [17]. They have numerous applications, such as anticancer [18], antibacterial [19], antiviral [20,21], antifungal [22], and their other biological properties [23].

Salicylaldimines, which are o-hydroxyl derivatives of azomethines, have piqued the interest of scientists due to a unique feature: an asymmetric intramolecular hydrogen bond between oxygen and nitrogen atoms[24]. Notably, azomethines generated from Salicylaldehyde variations with one or more halo atoms in their aromatic ring structure have demonstrated a wide range of intriguing biological actions. This occurrence emphasises the intriguing interaction between the chemical structure of the substance and its possible impact on biological systems [25]. Considering the therapeutic potential of azomethine derivatives, Schiff bases were synthesized from substituted salicyaldehyde and examined for their essential pharmacological properties. The primary goal of this study is to investigate these azomethines antibacterial, antimalarial, and antioxidant effects.

Experimental-

All chemicals and solvents were provided by Merck Pvt. Ltd. The 1H-NMR and 13C-NMR spectra were acquired using a BRUKER AVANCE III (500 MHz) spectrometer. Proton chemical shifts were referenced to tetramethylsilane, used as an internal standard, and measured in ppm. CHCl3 served as the solvent for these measurements. ESI-MS spectra were captured using a Waters Q-TOF MICROMASS spectrometer. Thin-layer chromatography (TLC) was conducted using E-Merck pre-coated aluminum sheets coated with fluorescent GF254 silica gel at a 0.2 mm layer thickness. This TLC method was employed for reaction monitoring and visualization was achieved using a UV-Visible cabinet.

General procedure for Schiff Base.

A solution of aromatic aldehyde (1 mmol) in hot methanol was slowly added dropwise to a hot methanolic solution of the corresponding substituted aromatic amines (1 mmol). The resulting reaction mixture was refluxed for 2-6 hours while being monitored using thin-layer chromatography. The formed colored solid was collected, washed with cold methanol, and subsequently recrystallized using an appropriate solvent [26].

P_1: (E)-4-((2-methyl-5-nitrophenyl imino) methyl) benzene-1, 3-diol

Yellow Crystals yield 83%. ^{1}H-NMR (DMSO, 500MHz) (δ, ppm): 13.18 (s, 1H, Ar-OH); 10.36 (s, 1H, Ar-OH); 8.85 (s, 1H, -C=N); 8.10 (s,1H, Ar-H); 7.99-7.97 (dd, 1H, Ar-H); 7.53-7.49 (dd, 2H, Ar-H); 6.44-6.42 (dd, 1H, Ar-H); 6.33 (d,1H, Ar-H); 3.37(S,3H,-CH3). ESI-MS: 273.29 (Obs) 272.26(Cal). ^{13}C-NMR (DMSO, 500MHz) (δ, ppm): 164.22; 163.23; 163.03;148.12; 146.79; 139.91; 134.81; 131.32; 120.16; 112.49; 111.98; 108.22; 102.26; 18.02.

P_2: (E)-4-((2, 6-difluorophenylimino) methyl) benzene-1, 3-diol.

Greenish Yellow, Crystals yield 83%. ^{1}H NMR (DMSO, 500MHz) (δ, ppm): 12.74 (s, 1H, Ar-OH); 10.42 (s, 1H, Ar-OH); 8.85 (s, 1H, -C=N); 7.50-7.49 (d, 1H, Ar-H); 7.27-7.20 (dd, 3H, Ar-

H); 6.44-6.22 (d,1H, Ar-H); 6.33(s,1H, Ar-H); 6.33 (d,1H, Ar-H). ESI-MS: 249.99 (Obs), 249.21 (Cal).^{13}CNMR (DMSO, 500MHz) (δ, ppm): 168.41, 163.22, 162.65, 155.89, 155.85, 153.92, 153.88, 134, 126.10-125.91, 112.29-111.93, 108.20, and 102.35.

P3: (E)-4-((2-chloro-5-methylphenylimino) methyl) benzene-1, 3-diol.

Yellow Crystals yield 87%. ^{1}H-NMR (DMSO,500 MHz) (δ, ppm): 13.72 (s, 2H, Ar-OH); 8.52 (s, 1H, -C=N); 7.34 (d, 1H, Ar-H); 7.28 (t,1H, Ar-H); 7.09 (d, 1H, Ar-H); 7.006 (dd, 1H, Ar-H); 6.48 (d, 1H, Ar-H); 6.45 (dd, 1H, Ar-H); 2.37 (s, 3H, -CH_3). ESI-MS: 262.33 (Obs), 261.70(Cal).^{13}C-NMR (DMSO, 500 MHz) (δ, ppm): 163.13; 163.09; 162.83; 144.24; 137.87; 134.64; 129.29; 127.95; 125.05; 119.89; 111.93; 107.99; 102.29; 20.43.

P_4: (E)-2-((3-bromo-4-fluorophenylimino) methyl) phenol.

Light Yellow crystals, Yeild-89%. ^{1}H -NMR ($CDCl_3$, 500MHz) (δ, ppm): 12.68 (s, 1H, Ar-OH); 8.54 (s, 1H, -C=N); 7.55-7.52 (t, 1H, Ar-H); 7.40-7.36 (dd, 2H, Ar-H); 7.03-6.99 (dd, 2H, Ar-H); 6.94-6.92 (dd, 2H, Ar-H). ESI-MS**:** 294.06 (**Obs**), 294.12(**Cal**). ^{13}C-NMR ($CDCl_3$,500MHz) (δ, ppm): 164.77; 160.07; 159.54; 157.59; 149.67; 149.60; 133.78-132.45, 119.56-119.08, 116.58; 109.67; 109.48; 105.54; 105.37.

P_5: (E)-5-(diethyl amino)-2-((2-mercapto-4-(tri fluoro methyl) phenyl imino) methyl) phenol-

Yellow crystals, Yeild-95%.^{1}H -NMR ($CDCl_3$,500MHz) (δ, ppm): 12.89 (s, 1H, Ar-OH); 8.46 (s,1H, -C=N); 7.66-7.64 (d, 1H, Ar-H); 7.35-7.32 (t, 1H, Ar-H); 7.25-7.22 (s,1H, Ar-H); 6.31-6.6.30 (t, 1H, Ar-H); 6.29-6.23 (t, 1H, Ar-H); 3.45-3.41 (m,4H, -CH_2); 1.24-1.21 (t, 6H, -CH_3); ESI-MS**:** 368.13 (Obs), 368.12 (Cal).^{13}C-NMR ($CDCl_3$, 500MHz) (δ, ppm)**:**163.06; 162.83; 146.64; 134.96; 134.13; 129.48; 127.60; 126.30; 125.24; 114.11; 108.45; 104.47; 96.53; 43.95 (2C); 12.42 (2C).

P_6: (E)-5-(diethyl amino)-2-((2-mercaptophenylimino) methyl) phenol.

Yellow crystals, ^{1}H-NMR ($CDCl_3$, 500MHz) (δ, ppm):13.27 (S, 1H, Ar-OH); 8.43 (S, 1H, -C=N); 7.62-7.61 (d, 1H, Ar-H); 7.24-7.09 (m, 4H, Ar-H); 6.26-6.23 (t, 2H, Ar-H); 3.04-3.39 (m, 4H, -CH_2); 1.2 (t,6H,-CH_3). ESI-MS: 300.09 (Obs), 300.42 (Cal). ^{13}C-NMR ($CDCl_3$,500MHz) (δ, ppm)**:**162.68, 161.65; 151.83; 146.21; 134.53; 129.48; 127.60; 126.25; 125.24; 117.48; 108.49; 104.07; 96.66; 43.89 (2C); 12.42 (2C).

P_7: (E)-3-((4-bromo-2-chlorophenylimino) methyl) benzene-1, 2-diol.

Reddish crystals, Yeild-98 %.^{1}H-NMR ($CDCl_3$,500MHz)(δ,ppm): 13.35 (s, 1H, Ar-H); 11.08 (s,1H, Ar-OH); 8.61 (s, 1H, -C=N); 7.66 (d, 1H, Ar-H); 7.47-7.45 (d, 1H, Ar-H); 7.16-7.15 (d, 1H, Ar-H); 7.15-7.13 (d, 1H, Ar-H); 7.04-7.0 (d,1H, Ar-H); 6.88-6.85 (t,1H, Ar-H). ESI-MS**:** 327.92 (Obs); 326.57(Cal).^{13}C-NMR ($CDCl_3$,500MHz) (δ, ppm): 165.26; 149.28; 145.61; 143.84; 131.90; 131.26; 129.56; 123.01; 121.38; 119.63; 119.40; 119.14; 118.94.

Antimicrobial Activity Protocol-

Antimicrobial activity of compound was examined by using the 'Broth Dilution Method' vurses three bacterial species like *Staphylococcus aureus*, *Pseudomonas aeruginosa*, *Escherichia coli* and three fungi species like *Aspergillus niger*, *Candida albicans*, *Aspergillus clavitus*. This method provides quantitative insights into antimicrobial efficacy. Inoculums size for each strain was standardized to 10^8 CFU/ml through turbidity comparison. Dimethyl sulfoxide (DMSO) was applied as a diluents. Sequential dilutions for primary and secondary screening were prepared.

The control, without antibiotics, was inoculated onto a suitable medium plate and left to incubate at 37°C overnight. The lowest compound concentration curbing organism growth after an overnight incubation was noted as the minimum inhibitory concentration (MIC).The compound was tested across concentration gradients: 1000 µg/ml, 500 µg/ml, 250 µg/ml, 200 µg/ml, 100 µg/ml, 50 µg/ml, 25 µg/ml, 12.5 µg/ml, and 6.250 µg/ml [27].

Antimalarial Activity Protocol-

Researchers used HEPES, glucose, sodium bicarbonate, and human serum to culture malaria-causing parasites in RPMI 1640. They created a controlled environment by mixing parasites and red blood cells in RPMI-1640, then adding test substances. The scientists observed the parasites' progression from rings to trophozoites and schizonts, which varied according on compound strength. This study gave light on how the tested chemicals could efficiently inhibit malaria parasite growth and advancement, providing viable disease-fighting techniques [28, 29].

Antioxidant Protocol

The antioxidant potential of azomethines (P1-P7) was evaluated by using the DPPH free radical scavenger test. In this method the compounds' capability to counteract damaging free radicals and compared their efficiency with known antioxidant BHT (butylated hydroxytoluene). DPPH solution dissolved in methanol was utilized. Various concentrations of the compounds dissolved in methanol (ranging from 5 -100 µg/ml) were mixed with a 0.004% DPPH solution. After a 30 minute incubation period at room temperature, a UV spectrophotometer measured the absorbance of light at 517 nm. This measurement provided an indication of how effective the test compounds were at controlling free radical formation from the DPPH solution. The percentage inhibition (I %) of free radical production from DPPH was determined using a specific formula. This test provided valuable insight into the potential antioxidant capabilities of the synthesized compounds and allowed for a direct comparison to BHT, a widely recognized antioxidant [30].

$$\% \text{ of Scavenging} = [(A_{\text{control}} - A_{\text{sample}})/A_{\text{blank}}] \times 100$$

A control = absorbance of the control reaction, and A sample = absorbance of azomethines.

Density Functional Theory

The DFT simulations were conducted in the gas phase utilizing the B_3LYP 6-311+ G (d,p) basis set. These calculations were performed using the ORCA program package (version 4.0.1) [31–33]. The methodology encompassed conducting geometrical optimization simulations for each prepared compound. This aimed to ascertain the most energetically favourable molecular structure and its corresponding frequencies, subsequently allowing the computation of various thermo chemical properties.

Molecular Docking-

Docking study using Auto Dock Vina assessed inhibition potentials of synthesized derivatives. Compounds were docked into binding sites of topoisomerase-II DNA gyrase crystal structure [34–37]. AutoDock Tools 1.5.4 (ADT) prepared input files, eliminating water molecules and ions, adding polar hydrogen via Kollman united charges method [38, 39]. PROPKA 2.0 assessed enzyme residue pKa values for nonstandard ionization states. Lysine, arginine, and histidine side chains were protonated; glutamic and aspartic acid carboxylic groups were deprotonated. Ligands underwent preparation: nonpolar hydrogen merge, Gasteiger charges, and rotatable bond setup. Structures saved as pdbqt files for AutoDock. A 40×40×40 Å grid box (x, y, and z) created around active pocket, centred on average crystallography ligand coordinates.

Result and Discussion-

Chemistry

Scheme 1 illustrates hydroxybenzaldehyde based Schiff bases. In the ^{1}H-NMR spectrum, the signal values of the -OH protons (2-position) inside the salicylaldimine ring involved in intramolecular hydrogen bonding with –C=N-nitrogen vary between 13.73-11.68 δ ppm. The ^{1}H -NMR signals of the second OH protons of P_1-P_3 (4-position) and P_7 (3-position) were obtained at below δ 10.10, 10.42, 13.72 and 13.35 δ ppm for P_1, P_2, , P_3 and P_7 respectively. The azomethine proton (-CH=N-) of compounds (P_1–P_7) appears in the range of δ 9.48–8.43 δ ppm. In ^{13}C-NMR spectra, the chemical shift of the azomethine carbon is observed at 162–168 δ ppm. ESI-MS peaks confirm the formation of Schiff bases (P1–P7) and assign molecular mass to the corresponding peaks[40].

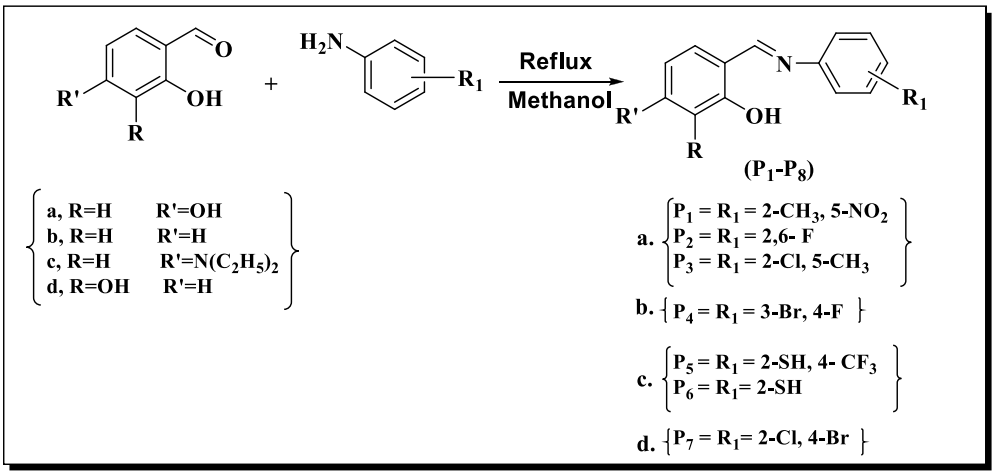

Scheme 1

Antibacterial activity-

An in vitro bactericidal study was conducted on procured compounds (P_1–P_7) against various bacterial strains, as summarised in Table 1. Among these derivatives, P_1 to P_3 and P_5 to P_6 exhibited sensible levels of activity, while P4 and P7 have restricted efficacy against *Escherichia coli* in comparison to Ampicillin. Regarding their impact on *Pseudomonas aeruginosa*, P_7 exhibited compatibility, while P_3, P_4, and P_5 indicated a moderate response, while the compounds P_1, P_2, and P_6 depicted inferior effects. Remarkably, these derivatives highlighted their most prominent efficiency against *Staphylococcus aureus*. Particularly, P_2 exhibited the most substantial activity (MIC = 25 µg/ml), whereas P_5 and P_6 displayed notably higher activity (MIC = 50–62.5 µg/ml). Furthermore, P_1, P_3, P_4, and P_7 illustrated enhanced efficacy against *Staphylococcus aureus* in comparison to Ampicillin. This finding holds significant importance given the opportunistic nature of *Staphylococcus aureus* as a pathogen, rendering compounds effective against it particularly valuable. The presence of fluorine (-F) and thiol (-SH) groups may contribute to the heightened activity against *Staphylococcus aureus*. Variations in the permeability of microbial cell structures or differences in microbial cell ribosomes likely underlie the variability in efficacy observed across various chemical agents against various bacterial species[41].

Table 1 Representation of Antibacterial Activity.

Compound Name	*E.coli*	*P.aeruginosa*	*S.aureus*
	MTCC 443	MTCC 1688	MTCC 96
P_1	125	250	100
P_2	100	250	25
P_3	100	125	125

P_4	250	125	100
P_5	100	125	62.5
P_6	125	500	50
P_7	250	100	250
Ampicillin	100	100	250

Antifungal activity-

In-vitro fungal inhibitory action of new azomethines (P_1-P_7) investigated against Aspergillus *niger*, *Candida albicans*, and *Aspergillus clavatus* and obtained outcome matched with the Greseofulvin drug. Compound P_1 and P_6 (250 μg/ml) exhibited enhanced activity against *Candida albicans*. Azomethines derivatives P_2 –P_5 and P_7 (500 μg/ml) depicted identical activity as Griseofulvin verses *Candida albicans* and inactive against Aspergillus *niger* and *Aspergillus clavatus*. The geometrical arrangement, polarity, and stability of compounds responsible for the different activity [42].

Table 2 Representation of Antifungal Activity.

Compound Name	*C.albicans* MTCC 227	*A. niger* MTCC282	*A.clavatus* MTCC 1323
P_1	250	500	--
P_2	500	--	--
P_3	500	--	--
P_4	500	--	--
P_5	500	--	--
P_6	250	--	--
P_7	500	500	500
Greseofulvin	500	100	100

Antimalarial activity

The antimalarial activity of azomethines (P_1-P_7) was tested against *P.falciparum* and compared with the quinine drug. In case of compound P_1, P_2, P_3, azomethine P_1 (IC_{50} = 0.47 μg/ml) show moderate activity, whereas ortho-fluoro-substituted analogue P_2 exhibited (IC_{50} = 1.45 μg/ml) inferior activity while P_3 shows weakly moderate activity. We can say that the existence of the electron-donating group at the ortho position of imines increases the activity, and the presence of the electron-withdrawing group decreases activity. In the case of Para-fluoro-substituted azomethines P_4 showed fair activity (IC_{50} = 0.61 μg/ml). Azomethine P_5 (0.29 μg/ml) exhibited good antimalarial activity due to $–CF_3$ substituent at the para positions, whereas in P_6 (1.38 μg/ml), this activity decreases due to the absence of $–CF_3$ group [15]. Compound P_7 exhibited

moderate activity because of the electron-withdrawing group at ortho with respect to the imine group. The antimalarial activity of these compounds acts in the following order, $P_5 > P_1 > P_4 > P_3 > P_7 > P_6 > P_2$.

Table 3 Representation of Antimalarial Activity.

Compound Name	Mean IC_{50} *P.Falciparum*
P-1	0.47 µg/ml
P-2	1.45 µg/ml
P-3	1.01 µg/ml
P-4	0.61 µg/ml
P-5	0.29 µg/ml
P-6	1.38 µg/ml
P-7	1.02 µg/ml
Quinine	0.268 µg/ml

Antioxidant activity

The antioxidant activity of the synthesized compounds was evaluated using a 1, 1-diphenyl-2-picrylhydrazyl (DPPH) radical scavenging assay. The presence of a phenolic OH group is obligatory for the creation of an active molecule, a property often observed in polyphenols. Prior research depicted that the positioning of hydroxyl groups within the Schiff bases considerably influences their antioxidant properties[43]. Remarkably, compound P_7 (14.26 µg/ml) illustrated robust antioxidant efficacy due to the presence of two OH groups in an ortho arrangement, intensifying the compound's efficacy. This contribution aligns with established literature on the correlation between the catechol moiety's structure and the antioxidant activity of polyphenols[44, 45]. On the other hand, Compounds P_1, P_2, and P_3 (IC_{50} µg/ml) exhibited modest antioxidant activity, attributed to the meta-substituted positioning of two OH groups[16]. In contrast, P_4, P_5, and P_6 exhibited notable antioxidant activity attributed to the ortho-substituted OH group. The antioxidant activity of P_4 and P_5 slightly diminished due to the electron-withdrawing effect at the para position of the imines group in comparison to P_6 [46].The derived values imply a hierarchy of compound activity as follows: $P_7 > P_6 >$ BHT $> P_5 > P_4 > P_1 > P_3 > P_2$. These findings shed light on the order of efficacy among these compounds, providing insights into their antioxidant potential.

Table 4 Representation of Antioxidant Activity.

Compound Name	Antioxidant activity. IC_{50}(µg/mL)
P_1	27.21± 0.38

P_2	31.92± 0.03
P_3	37.10± 0.77
P_4	19.05 ± 0.12
P_5	18.26± 0.24
P_6	16.32 ± 0.51
P_7	14.26± 0.37
BHT	16.47± 0.18

DFT Calculations Studies

Figures 1–7 depicts the optimised molecular structures of procured azomethine derivatives (P1–P7). The compounds P_1, P_3, P_5 and P_6 showed non-planar properties in contrast to P_2, P_4 and P_7. This non-planarity is maintained by the lack of imaginary frequencies, demonstrating stability.

A DFT result compiles in **Table 5** with thermal parameters and dipole moments calculations across compounds P_1 to P_7. Among these findings, it is evident that the dipole moments in the gas phase are as follows: 10.801 (P_1), 3.981 (P_2), 3.860 (P_3), 4.571 (P_4), 8.329 (P_5), 4.589 (P_6), and 5.758 (P_7) in Debye units. The substantial dipole moments of P_1 and P_5 contribute to strong intramolecular interactions. Subsequently, these compounds (P_1 and P_5) exert a significant impact on the binding positions of specific target proteins[47].

Frontier Molecular Orbital's

The highest occupied molecular orbital (HOMO) and the lowest unoccupied molecular orbital (LUMO) are collectively called as frontier molecular orbital's (FMOs).The frontier MOs calculations have been applied to understand the electronic excitation properties. Classically, the HOMO functions as an electron donor, associated with the ionization potential, whereas the LUMO acts as an electron acceptor, dependent upon the electron affinity of the molecule [48, 49]. Frontier molecular orbital's play an essential role in regulating the binding interactions between pharmaceutical compounds and receptor molecules and provide qualitative insights into the probability of electron migration from the HOMO to the LUMO. Recent scientific study have underscored the linkage between FMOs of drug molecules and the exploration of diverse biological activities, such as anticancer [50, 51], antifungal [52], antimicrobial, and cytotoxicity [53]. This correlation holds substantial promise within the realm of innovative drug design [54]. In the present study, the frontier molecular orbitals of the evaluated compounds P_1 to P_7 were computed using the DFT B3LYP/6–311+G (d, p) method to juxtapose the energy levels of HOMO and LUMO. Figures 8–14 portray the computed three-dimensional density surface plots delineating the FMOs of the examined compounds (P_1–P_7) as well as their HOMOs and LUMOs. The resulting

outcomes are summarized in Table 5. The energy levels of the HOMOs from -5.1384 to -6.0688; conversely, the LUMOs -0.7807 to -2.5165 eV, dependent upon the extent of conjugation and the atomic environments adjacent to the nucleus. Moreover, the energy gap (ΔE) of azomethine derivatives lies within the range of ΔE = 3.4627–4.3577 eV. Particularly, the compounds P_1 and P_4 exhibit elevated HOMO energy levels of E_{HOMO} = -5.9792 and -6.0688 eV, representing potent electron donors. Among these, compound P_1 emerges as an exceptional electron acceptor with an E_{LUMO} of -2.5165 eV. This judgment indicates the heightened binding affinity of compound P_1 relative to its counterparts. Furthermore, azomethine P_1, characterized by a reduced energy gap (ΔE = 3.4627 eV) between its FMOs, substantiates its pronounced binding affinity, thereby facilitating the engagement of drug molecules with receptors[55].

Chemical Reactivity Descriptors

The frontier molecular orbital's (FMOs) utilized to evaluate chemical reactivity descriptors, including traits such as electronegativity (χ), global hardness (η), softness (δ), and electrophilicity (ω). Therefore, the FMOs of azomethine P_1 to P_7 are used to speculate extra chemical reactivity descriptors that include ionization potential ($I = E_{HOMO}$) and electron affinity ($A = E_{LUMO}$). Chemical hardness (η) is closely related to the stability and reactivity of a given chemical system. According the frontier molecular orbital concept, the chemical hardness (η) corresponds to the energy gap between the HOMO and LUMO. As the energy gap increases, the molecule adopts greater hardness and stability, thereby exhibiting diminished reactivity. Remarkably, compound P_3 features an especially wider energy gap, suggesting superior hardness. Elevated energy gap values denote the augmented hardness or reduced softness of a compound. Consequently, P_3 assumes the profile of a rigid molecule, thereby establishing a hierarchy of relative stability as follows: $P_3 > P_2 > P_4 > P_7 > P_6 > P_5 > P_1$. In contrast, compound P_1 emerges as more reactive and less stable due to its narrower energy gap. Another pivotal global reactivity descriptor, the electrophilicity index (ω), offers a lucid portrayal of a system's propensity to accept electrons. Elevated electrophilicity index values correspond to heightened electron-accepting capabilities within these systems. Compound P_1 is distinguished by a substantial electrophilicity index value (5.2114 eV), underscoring its augmented electron acceptance when compared to other compounds (P_2-P_7). Conversely, compound P_3 exhibits diminished electron-accepting capacity due to its lower electrophilicity index (2.0 eV).Compound P_1 further stands out with an elevated basicity (χ = 4.2478 eV) relative to the other compounds, potentially contributing to its heightened binding affinity.

Table 5: Calculated electronegativity (χ), global hardness (η), softness (δ), global electrophilicity index (ω), the ionization potential (I), and the electron affinity (A) (in eV) of investigated compounds P_1 to P_7.

Parameters	P_1	P_2	P_3	P_4	P_5	P_6	P_7
E_{Tot} (Hartree)	-950.70	-905.40	-1205.65	-3304.12	-1579.39	-1242.37	-3739.65
Total Dipole Moment (Debye)	10.801	3.981	3.860	4.571	8.329	4.589	5.758
E_{HOMO} (eV)	-5.9792	-5.6901	-5.1384	-6.0688	-5.3953	-5.1733	-5.9513
E_{LUMO} (eV)	-2.5165	-1.5855	-0.7807	-1.9658	-1.6579	-1.2968	-1.9974
ΔE (eV)	3.4627	4.1046	4.3577	4.1030	3.7374	3.8765	3.9539
χ	4.2478	3.6378	2.9595	4.0173	3.5266	3.2351	3.9743
η	1.7312	2.0523	2.1788	2.0515	1.8687	1.9382	1.9769
δ	0.5775	0.4872	0.4589	0.4874	0.5351	0.5159	0.5058
ω	5.2114	3.2241	2.0099	3.9333	3.3277	2.6999	3.9949
I	5.9792	5.6901	5.1384	6.0688	5.3953	5.1733	5.9513
A	2.5165	1.5855	0.7807	1.9658	1.6579	1.2968	1.9974

P_1

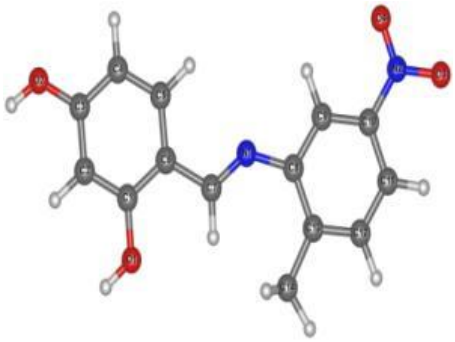

Figure 1

P_2

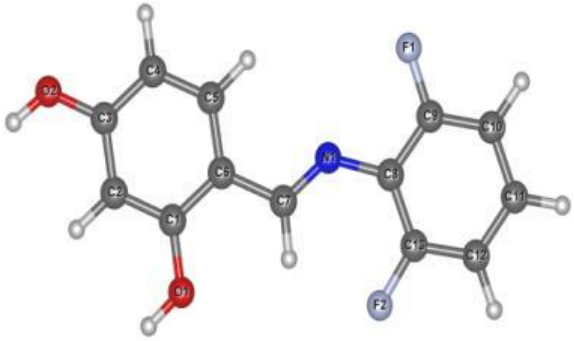

Figure 2

P_3

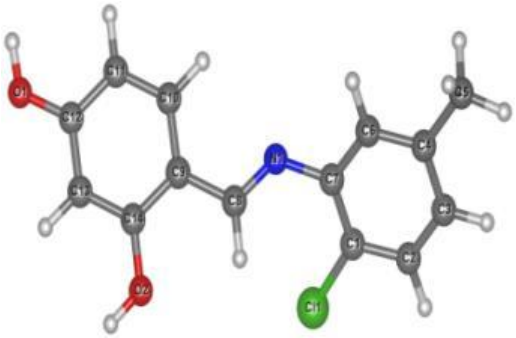

Figure 3

P_4

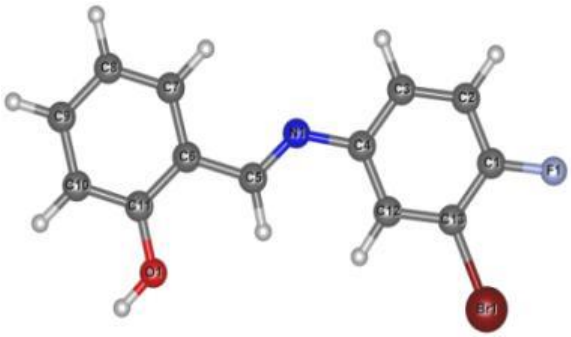

Figure 4

P_5

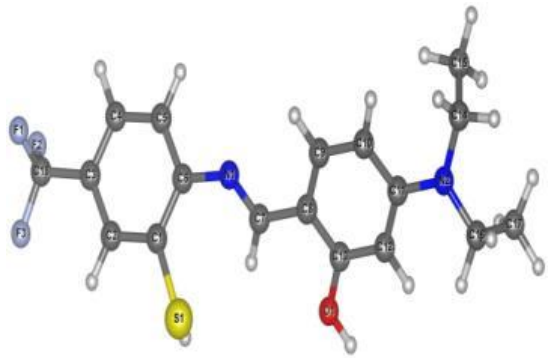

Figure 5

P_6

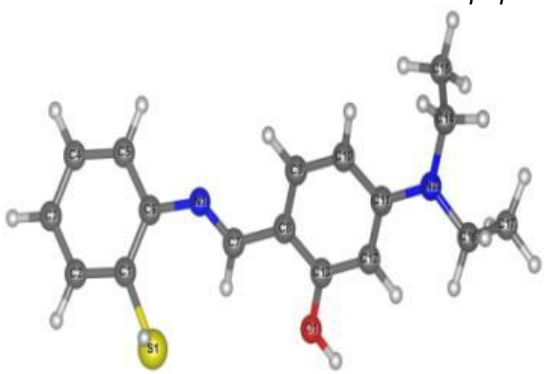

Figure 6

P_7

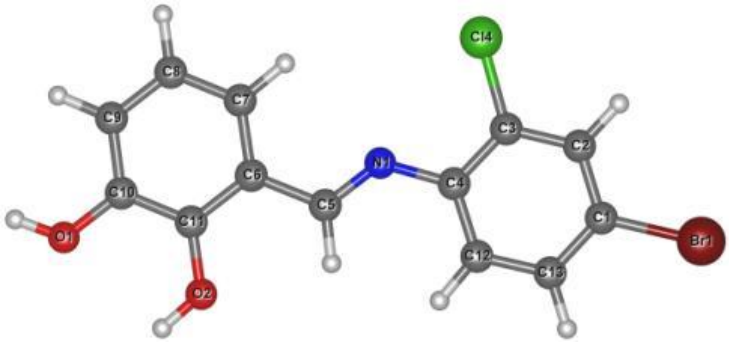

Figure 7

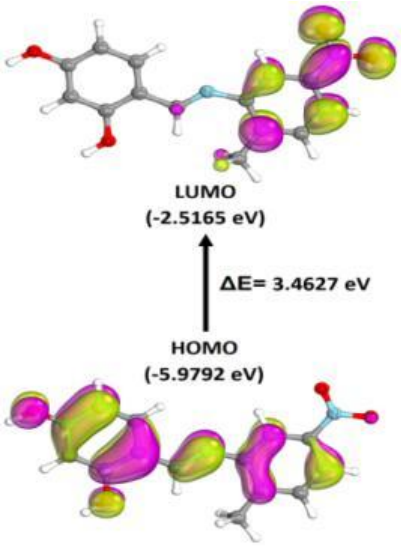

Figure 8

P_1

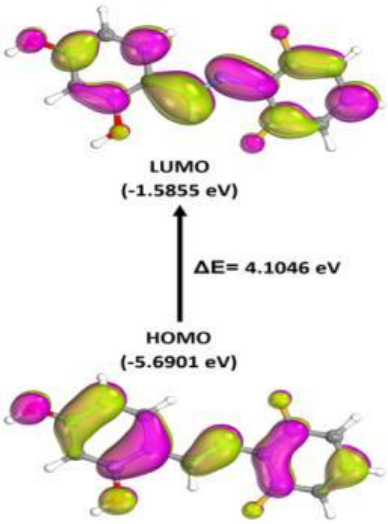

Figure 9

P_2

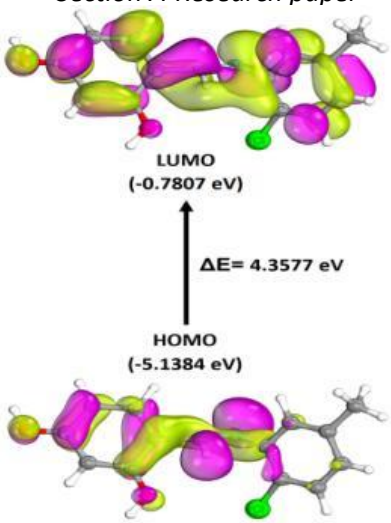

Figure 10

P_3

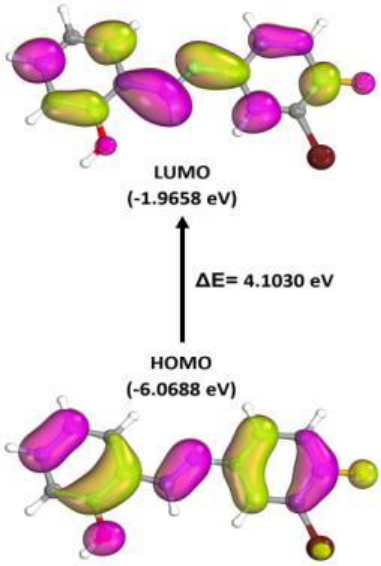

Figure 11

P_4

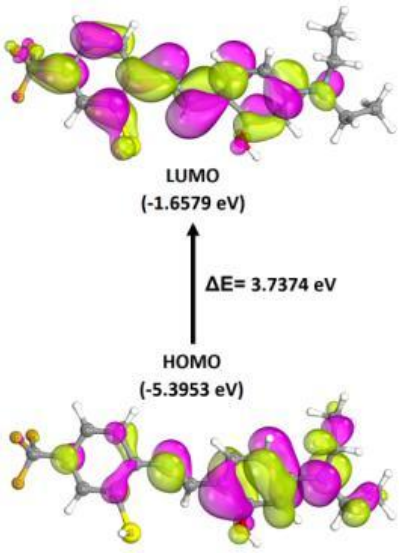

Figure 12

P_5

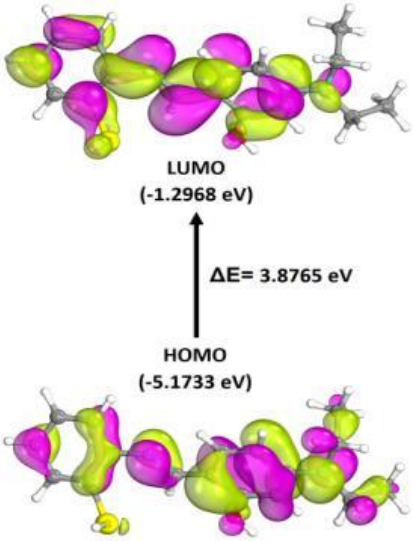

Figure 13

P_6

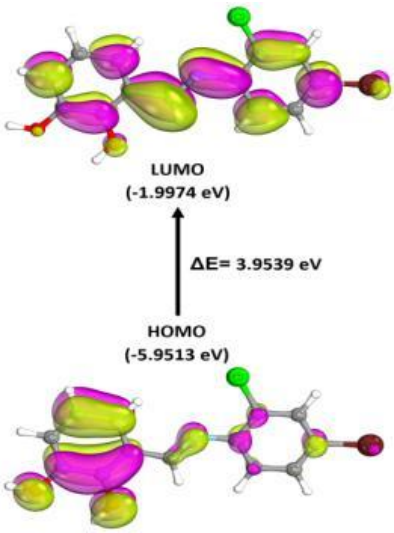

Figure 14
P_7

Molecular Docking-

To determine the antibacterial potential of synthesized compounds molecular docking study was carried out against *S.aureus* using topoisomerase II DNA gyrase enzymes results are shown in (Table 6). All the Synthesized compounds show docking active sites of topoisomerase II DNA gyrase. Among them, P_2 (-5.188 Kcal/mol), P_5 (-5.168 Kcal/mol), and P_1 (-5.077 Kcal/mol) are the most active as per the result in the molecular docking study. All active derivatives very efficiently bind in topoisomerase II DNA gyrase's active site into residues like ASP1083, SER1084, GLU1088, Arg1122, DG8, DG9, DC13and DC12, respectively.

Table 6 Representation of Molecular docking of synthesized derivatives

Compounds	Free Binding Energy (Kcal/mol)
P_1	-5.077
P_2	-5.188
P_3	-4.2916
P_4	-4.3258
P_5	-5.168
P_6	-4.5269
P_7	-4.0955
CCPX	-5.0837

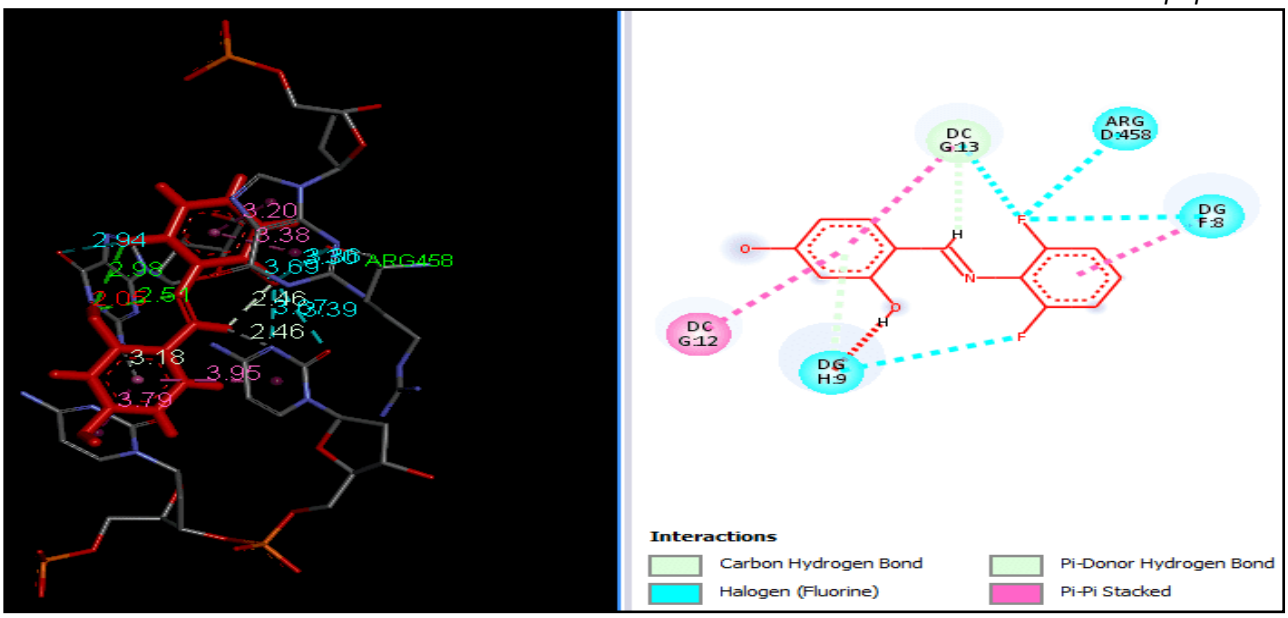

Figure 15 Binding Pose and molecular interactions of P_2

The compound P_2 (-5.188 Kcal/mol) interacts with positively Charged amino acid residues ARG458 to show carbon-fluorine interaction with a distance of 3.30Å. The Deoxy-cytosine Nucleotide base pairs DC13 and DG8 interact with –F to show carbon-fluorine interaction with the distance of 3.39 and 3.36Å, respectively. Nucleotide base pairs Deoxycytosine DC13 and DC12 interact with Pi-electron clouds aromatic resorcinol imine ring to form Pi-Pi stacked with a distance of 3.20 and 3.38 Å, respectively. Nucleotide base pairs Deoxycytosine DC13 interrelate with the imine hydrogen atom of the imine bridge to show carbon-hydrogen bond interaction with a distance of 2.46Å shown in Figure 15. Azomethine P_5 (-5.168 Kcal/mol) interacts with positively charged amino acid ARG 458 with –OH hydrogen atom of phenyl ring with a distance of 2.08 to form conventional carbon-hydrogen bond interactions, whereas it also interacts with fluorine atoms of $-CF_3$ substitute to form conventional carbon-hydrogen bond interactions with the distance of 3.31 and 3.69Å respectively. The positively charged amino acid ARG1122 interacts with the hydrogen atom of $-CH_3$ to form carbon-hydrogen bond interactions with a distance of 2.53Å. Nucleotide base pairs Deoxygenosine DG8, DG9, and Deoxycytosine DC12, DC13 interact with N, N- diethyl side chain,-SH, and Pi electron clouds of the phenyl ring to form a carbon-hydrogen bond, Pi-donor hydrogen bond interactions, Pi-Pi Stacked and Pi-alkyl interactions (Figure 16).

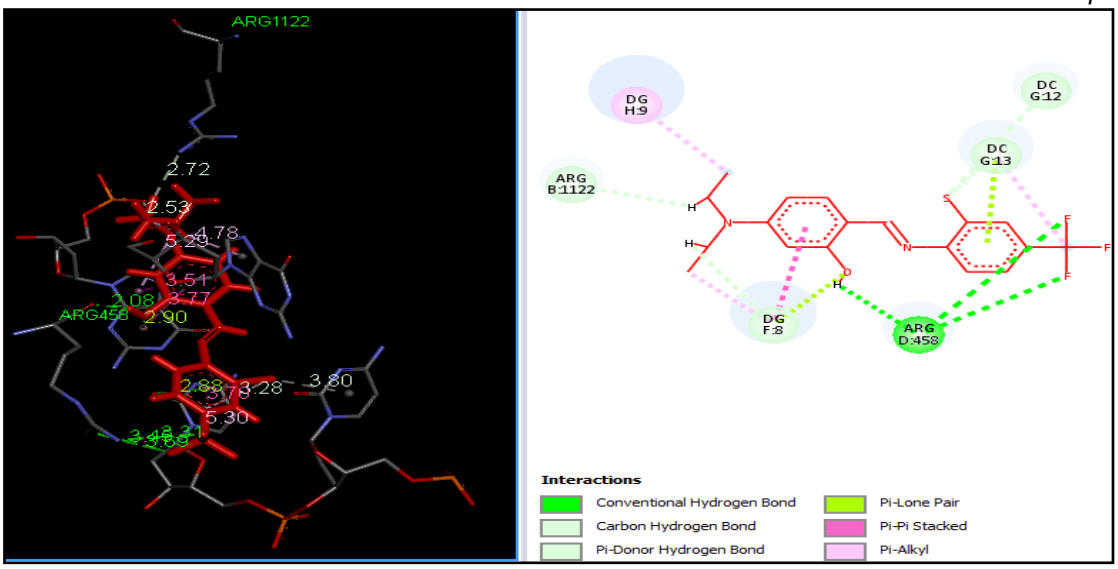

Figure 16 Binding Pose and molecular interactions of P_5.

The synthesized compounds P_1 (-5.077Kc al/mol) interact with the Nucleotide base pair Deoxycytosine DC09 to form conventional hydrogen bond interaction and Pi-lone pair interactions with the hydrogen atom of the oxygen atom of the Nitro group with the distance of 3.37 Å. It also interacts with the electron cloud of aromatic resorcinol imine ring with a distance of 3.33Å. Other Nucleotide base pairs, Deoxycytosine DC12 and Deoxycytosine DC12, interact with the π electron cloud of aromatic resorcinol imine ring and alkyl substitute $–CH_3$ group with a distance of 3.62, 3.64, and 4.84Å to show Pi-Pi Stacked and Pi-alkyl interactions. Deoxygenosine DG8 interact with the π electron cloud of the phenyl ring and $–CH_3$ group to form π-π stacked and π-alkyl interactions of various distance shown in Figure 17.

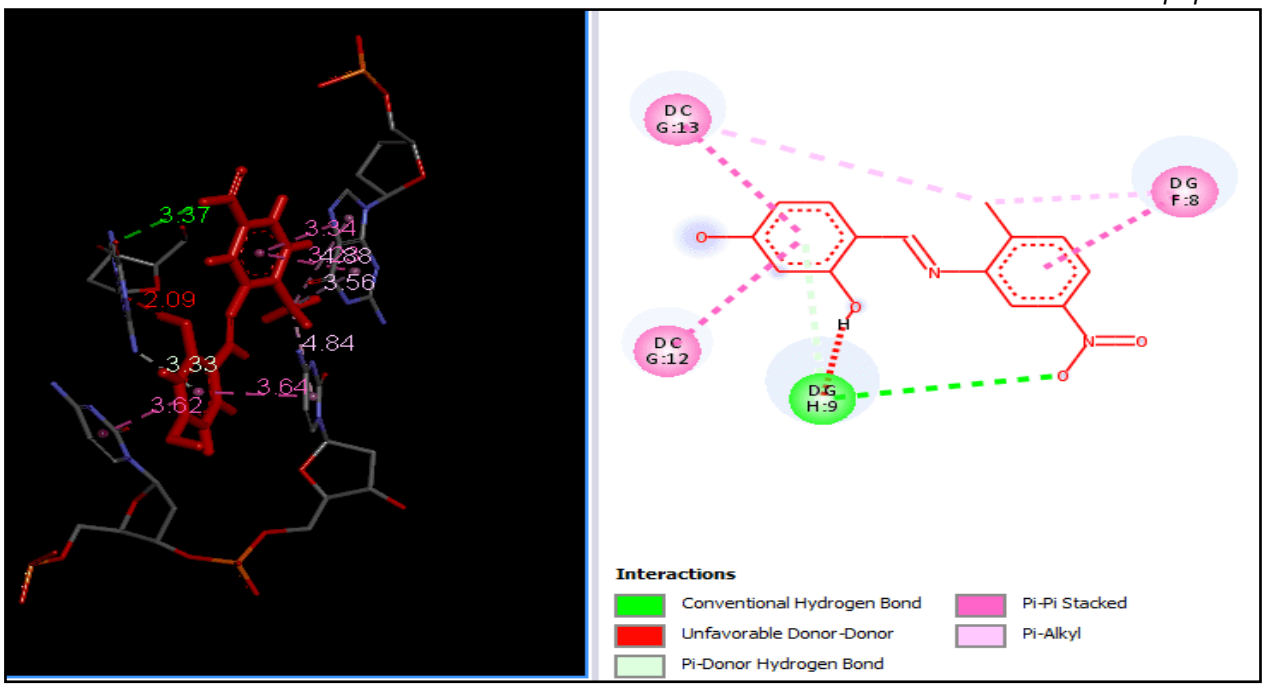

Figure 17 Binding Pose and molecular interactions of P_1.

Conclusion

All synthesized compounds exhibited moderate to suitable biological activities, antioxidant, antimalarial, antibacterial, and antifungal. *In-vitro* and *In-silico* study confirms that azomethine P_2 are excellent lead in antimicrobial drug against *Staphylococcus aureus* with a binding energy of -5.188 Kcal/mol as compared standard drug ciprofloxacin. This research demonstrates that the procured compounds can effectively discontinue bacterial growth. The compound P_5 showed noteworthy antimalarial activity, while compound P_7 exhibited significant antioxidant activity. The *in-silico* investigation suggests that P_1 (-5.077 Kcal/mol), P_2 (-5.188 Kcal/mol), and P_5 (-5.168 Kcal/mol) have the higher activity. However, the DFT analysis shows that compounds P_1 and P_5 display a reduced energy gap and a bigger dipole moment. These characteristics indicate a high binding affinity but also decreased stability, increased reactivity, and increased basicity. These properties improve these compounds' capacity to interact with drug receptors. Combining computational and biological investigations, we can determine that compound P_5 stands out as the mainly biologically active compound within the synthesized set of compounds. It shows antioxidant capacity at 18.26 µg/ml, remarkable antimalarial potency 0.29 µg/ml and notable antibacterial efficacy of 62.5 µg/ml. At the same time, P_1 has good antifungal and moderate antimalarial activity. Among all compounds P_3 is the most stable with less dipole moment and a high energy gap hence P_3 is biologically less active.

Acknowledgment-

The authors express their gratitude to the Department of Science and Technology for providing research facilities via the DST-FIST programme (Project NO-SR/FIST-415/2018). The authors gratefully appreciate SAIF Punjab University. The authors would also like to express their gratitude to the honourable Management, Principal, and Head of the Department of Chemistry of KKHA Arts, SMGL Commerce, and SPHJ Science College Chandwad for their research assistance.

Disclosure statement. The author disclosed no potential conflicts of interest.

References-

1 W. Gao, S. Thamphiwatana, P. Angsantikul and L. Zhang, *WIREs Nanomedicine and Nanobiotechnology*, **6**, 532–547, (2014).

2 A. Tagliabue and R. Rappuoli, *Frontiers in Immunology*, 9, 1068, (2018).

3 A. S. Hassan, A. A. Askar, A. M. Naglah, A. A. Almehizia and A. Ragab, *Molecules*, 25(11), 2593, (2020)

4 S. K. Nandanwar and H. J. Kim, *Chemistry Select*, **4**, 1706–1721, (2019).

5 R. Muthukumar, M. Karnan, N. Elangovan, M. Karunanidhi and R. Thomas, *Journal of the Indian Chemical Society*, **99**, 100405, (2022).

6 K. J. Rajimon, N. Elangovan, A. Amir Khairbek and R. Thomas, *Journal of Molecular Liquids*, **370**, 121055, (2022).

7 R. S. Bendre, R. D. Patil, P. N. Patil, H. M. Patel and R. S. Sancheti, *Journal of Molecular Structure*, **1252**, 132152, (2022).

8 M. S. More, P. G. Joshi, Y. K. Mishra and P. K. Khanna, *Materials Today Chemistry*, **14**, 100195, (2019)

9 B. Ames, M. Shigenaga and T. O. HAGEN, *and the degenerative diseases of aging. Proceedings of the National Academy of Sciences of the United States of America*, **90**, 7915–7922, (1993)

10 G. A. Engwa, *Phytochemicals: Source of Antioxidants and Role in Disease Prevention. BoD–Books on Demand*, **7**, 49–74,(2018)

11 L. I. Socea, D. C. Visan, S. F. Barbuceanu, T. V. Apostol, O. G. Bratu and B. Socea, *Rev Chim (Bucharest)*, **69**, 795–797, (2018)

12 M. Taghvaei and S. M. Jafari, *Journal of food science and technology*, 2015, **52**, 1272–1282.

13 L.-X. Cheng, J.-J. Tang, H. Luo, X.-L. Jin, F. Dai, J. Yang, Y.-P. Qian, X.-Z. Li and B. Zhou, *Bioorganic & Medicinal Chemistry Letters*, **20**, 2417–2420, (2010)

14 World Health Organization, *World Malaria Report* , World Health Organization, 2012.

15 M. Sharma, K. Chauhan, R. K. Srivastava, S. V. Singh, K. Srivastava, J. K. Saxena, S. K. Puri and P. M. Chauhan, *Chemical biology & drug design*, **84**, 175–181, (2014)

16 K. S. Munawar, S. M. Haroon, S. A. Hussain and H. Raza, *J Basic Appl Sci*, 2018, **14**, 217–229.

17 D. Sinha, A. K. Tiwari, S. Singh, G. Shukla, P. Mishra, H. Chandra and A. K. Mishra, *European journal of medicinal chemistry*, **43**, 160–165,(2008)

18 N. Uddin, F. Rashid, S. Ali, S. A. Tirmizi, I. Ahmad, S. Zaib, M. Zubair, P. L. Diaconescu, M. N. Tahir and J. Iqbal, *Journal of Biomolecular Structure and Dynamics*, **38**, 3246–3259,(2020)

19 K. H. M. E. Tehrani, M. Hashemi, M. Hassan, F. Kobarfard and S. Mohebbi, *Chinese Chemical Letters*, **27**, 221–225, (2016)

20 A. Jarrahpour, P. Shirvani, H. Sharghi, M. Aberi, V. Sinou, C. Latour and J. M. Brunel, *Medicinal Chemistry Research*, **24**, 4105–4112, (2015)

21 S. Y. Abbas, A. A. Farag, Y. A. Ammar, A. A. Atrees, A. F. Mohamed and A. A. El-Henawy, *Monatshefte für Chemie-Chemical Monthly*, **144**, 1725–1733, (2013)

22 C. Wang, L. Fan, Z. Pan, S. Fan, L. Shi, X. Li, J. Zhao, L. Wu, G. Yang and C. Xu, *Molecules*, **27**, 6858, (2022)

23 W. Al Zoubi, A. A. S. Al- Hamdani, S. D. Ahmed and Y. G. Ko, *Journal of Physical Organic Chemistry*, **31**, e3752, (2018)

24 A. Cinarli, D. Gürbüz, A. Tavman and A. S. Birteksöz, *Chinese Journal of Chemistry*, **30**, 449–459, (2012)

25 L. C. Felton and J. H. Brewer, *Science*, **105**, 409–410, (1947)

26 R. S. Bendre, R. D. Patil, P. N. Patil, H. M. Patel and R. S. Sancheti, *Journal of Molecular Structure*, **1252**, 132152, (2022)

27 S. K. Tadavi, A. A. Yadav and R. S. Bendre, *Journal of Molecular Structure*, **1152**, 223–231, (2018)

28 C. J. Paniker, *Textbook of medical parasitology.*, Jaypee Brothers Medical Publishers (P) Ltd, 2007.

29 C. Lambros and J. P. Vanderberg, *The Journal of parasitology*, 418–420, (1979)

30 U. K. Sharma, S. Sood, N. Sharma, P. Rahi, R. Kumar, A. K. Sinha and A. Gulati, *Medicinal Chemistry Research*, **22**, 5129–5140, (2013)

31 F. Neese, *Wiley Interdisciplinary Reviews: Computational Molecular Science*, **8**, e1327, (2018)

32 R. Krishnan, J. S. Binkley, R. Seeger and J. A. Pople, *The Journal of chemical physics*, **72**, 650–654, (1980)

33 A. McLean and G. Chandler, *The Journal of chemical physics*, **72**, 5639–5648, (1980)

34 B. D. Bax, P. F. Chan, D. S. Eggleston, A. Fosberry, D. R. Gentry, F. Gorrec, I. Giordano, M. M. Hann, A. Hennessy, M. Hibbs, J. Huang, E. Jones, J. Jones, K. K. Brown, C. J. Lewis, E. W. May, M. R. Saunders, O. Singh, C. E. Spitzfaden, C. Shen, A. Shillings, A. J. Theobald, A. Wohlkonig, N. D. Pearson and M. N. Gwynn, *Nature*, **466**, 935–940, (2010)

35 T. Ponnusamy, M. Alagumuthu and S. Thamaraiselvi, *Bioorg Med Chem*, **26**, 3438–3452.

36 S. Uzun, Z. Demircioğlu, M. Taşdoğan and E. Ağar, *Molecular Crystals and Liquid Crystals*, 2022, **742**, 25–39, (2018)

37 P. Subbaraj, A. Ramu, N. Raman and J. Dharmaraja, *Journal of Coordination Chemistry*, **67**, 2747–2764, (2014)

38 O. Trott and A. J. Olson, *Journal of Computational Chemistry*, **31**, 455–461, (2014)

39 G. M. Morris, R. Huey, W. Lindstrom, M. F. Sanner, R. K. Belew, D. S. Goodsell and A. J. Olson, *Journal of Computational Chemistry*, **30**, 2785–2791, (2009)

40 D. C. Bas, D. M. Rogers and J. H. Jensen, *Proteins: Structure, Function, and Bioinformatics*, **73**, 765–783, (2008)

41 A. A. Shanty, J. E. Philip, E. J. Sneha, M. R. Prathapachandra Kurup, S. Balachandran and P. V. Mohanan, *Bioorganic Chemistry*, **70**, 67–73, (2017)

42 T. Y. Fonkui, M. I. Ikhile, P. B. Njobeh and D. T. Ndinteh, *BMC Chemistry*, 2019, **13**, 127.

43 Z. D. Petrović, J. Đorović, D. Simijonović, V. P. Petrović and Z. Marković, *RSC Advances*, **5**, 24094–24100, (2015)

44 P. Trouillas, P. Marsal, D. Siri, R. Lazzaroni and J.-L. Duroux, *Food Chemistry*, **97**, 679–688, (2006)

45 D. Kozlowski, P. Trouillas, C. Calliste, P. Marsal, R. Lazzaroni and J.-L. Duroux, *The Journal of Physical Chemistry A*, **111**, 1138–1145, (2007)

46 B. Vhanale, D. Kadam and A. Shinde, *Heliyon*, **8**, e09650, (2022)

47 M. Kouza, A. Banerji, A. Kolinski, I. Buhimschi and A. Kloczkowski, *Molecules*, **23**, 1995, (2018)

48 Y. Deswal, S. Asija, A. Dubey, L. Deswal, D. Kumar, D. K. Jindal and J. Devi, *Journal of Molecular Structure*, **1253**, 132266, (2022)

49 A. Nataraj, V. Balachandran, T. Karthick, M. Karabacak and A. Atac, *Journal of Molecular Structure*, **1027**, 1–14, (2012)

50 M. Hagar, H. Ahmed, T. El-Sayed and R. Alnoman, *Journal of Molecular Liquids*, **285**, 96–105,(2019)

51 A. I. Khodair, M. K. Awad, J.-P. Gesson and Y. A. Elshaier, *Carbohydrate research*, **487**, 107894, (2020)

52 R. Joshi, A. Kumari, K. Singh, H. Mishra and S. Pokharia, *Journal of Molecular Structure*, **1206**, 127639, (2020)

53 R. M. da Costa, J. K. Bastos, M. C. Costa, M. M. Ferreira, C. S. Mizuno, G. F. Caramori, G. R. Nagurniak, M. R. Simão, R. A. Dos Santos and R. C. Veneziani, *Phytochemistry*, **156**, 214–223, (2018)

54 D. F. Lewis, *Inflammopharmacology*, **11**, 43–7, (2003).

55 A. Al Sheikh Ali, D. Khan, A. Naqvi, F. F. Al-Blewi, N. Rezki, M. R. Aouad and M. Hagar, *ACS omega*, **6**, 301–316, (2020)